J Sol-Gel Sci Technol (2017) 83:609–617
DOI 10.1007/s10971-017-4466-0

ORIGINAL PAPER: NANO-STRUCTURED MATERIALS (PARTICLES, FIBERS, COLLOIDS, COMPOSITES, ETC.)

Template-free fabrication of hierarchically meso/macroporous architecture of layered double hydroxide by dry gel conversion method

Jingjing Han[1] · Rong Zhang[1] · Yue Zhang[1] · Fazhi Zhang[1]

Received: 25 April 2017 / Accepted: 5 July 2017 / Published online: 18 July 2017
© Springer Science+Business Media, LLC 2017

Abstract A new type of hierarchically porous architecture of Mg^{2+}, Al^{3+}-containing layered double hydroxide, with well defined mesoporous/macroporous structure, has been fabricated by dry gel conversion method without the need of a surfactant and organic solvent. Predefined amorphous aluminum hydroxide gel and anhydrous magnesium sulfate were used as Al and Mg precursor material, respectively, and aqueous ammonia as precipitating agent. The resulting self-sustaining hierarchical layered double hydroxide material exhibits a bi-modal porous structure having a macroporous network with macropore sizes of 100–200 nm and a well defined mesoporous structure of pore size around 3.9 nm in the macroporous framework. Layered double hydroxide crystallites are aligned with a multilayer manner to form the architecture structure. The formation process of layered double hydroxide architecture, such as the evolution of phase composition, pore structure, and particle morphology with reaction time was further verified and the formation mechanism is postulated.

Graphical Abstract

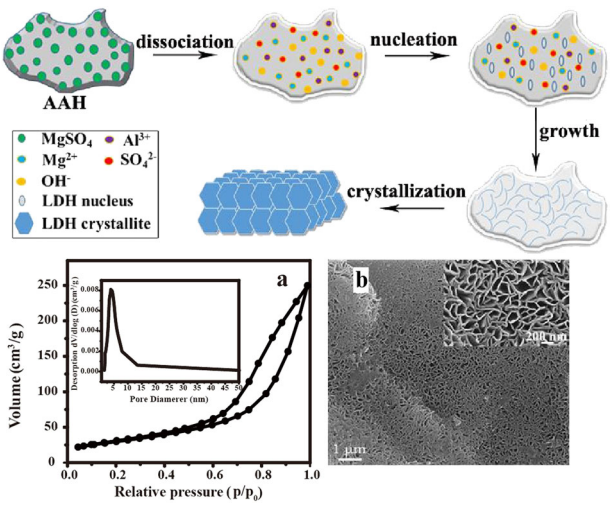

Keywords Layered double hydroxide · Hierarchical porous · Self-sustaining · Dry gel conversion

1 Introduction

Layered double hydroxides (LDHs), also known as anionic clays, have attracted increasing interest due to their potential industrial applications in areas, such as catalysis, separation, adsorption, additives in polymers, drug delivery, environmental remediation, and energy storage [1–4]. For the typical structure of LDHs, whose general chemical composition is $[M^{2+}_{1-x}M^{3+}_{x}(OH)_2]A^{n-}_{x/n}\cdot mH_2O$, the metal octahedra share edges to form 2D infinite sheets with similar structure to that of brucite $[Mg(OH)_2]$. The identities of the M^{2+} and M^{3+} cations in brucite-like layer and the

Electronic supplementary material The online version of this article (doi:10.1007/s10971-017-4466-0) contains supplementary material, which is available to authorized users.

Jingjing Han and Rong Zhang authors are contributed equally to this work.

✉ Fazhi Zhang
zhangfz@mail.buct.edu.cn

[1] State Key Laboratory of Chemical Resource Engineering, Beijing University of Chemical Technology, Beijing 100029, China

interlayer anions A^{n-}, together with the value of the stoichiometric coefficient x, can be varied over a wide range, allowing LDH materials to be fabricated with a wide variety of properties.

LDHs are generally prepared by coprecipitation method, consisting of mixing divalent and trivalent metal salts in aqueous solution at constant or variable pH followed by aging at a certain temperature. The resulting LDH powders typically show the anisotropic platelet morphology in which the dimensions of the (typically hexagonal) *ab*-faces of the platelets are much larger than the thickness (the dimension along the *c*-axis) of the platelets. The sheet-like LDH crystallites are often observed to aggregate during crystallization, storage and application, due to the high surface energy. For the purpose of migrating such crucial aggregation problem, a special attention has been drawn to the preparation of hierarchical architectures of LDHs from the last decade [5, 6]. Commonly, soft-templating and hard-templating syntheses are presently the two most widely used methods. In the former case, various surfactants or polymers have been adopted as soft templates for controlling the LDH nanostructures by forming spherical micelles or microemulsions [7–9]. In the case of hard-templating process, hollow LDH spherical architectures were fabricated by using polystyrene latex, carbon or silica as hard cores [10–12], and positively charged colloidal LDH nanoplatelets were deposited as building block on the core surface followed by removal of the template via calcination or dissolution. Besides, a three-dimensional open macroporous LDH framework was prepared during a process of coprecipitation with the polystyrene sphere colloidal crystal template, which presented an unusual bimodal structure displaying both mesopores and macropores [13, 14]. However, the hard-template method suffers from problems of materials compatibility and process complexity, and the soft-template technique often require a lot of organic solvent to deal with, which is neither convenient nor environmental friendly. Developing of template-free approach under mild conditions is highly desired and still remains a challenge for the controlled fabrication of LDH architectures.

Herein, we report on the facile preparation of LDH hierarchically mesoporous/macroporous architectures by means of a dry gel conversion (DGC) procedure. Indeed, hierarchically porous materials with bi-modal or multimodal of porosities have currently attracted considerable attention for their potential applications, in view of their allowing easy diffusion of guest molecules of different sizes through pore channels of different length scales among the inorganic frameworks [15, 16]. So far several classes of microporous or mesoporous crystal materials have been fabricated by DGC technique, such as zeolites [17–21], dense zeolite coatings [22, 23] and metal-organic frameworks [24]. The solvent water necessary for DGC (and sometimes with structure-directing agent or organic template) is kept separate from the gel solids in the autoclave during reaction. Because a small amount of solvent is used for the synthesis, DGC allows significant reductions of reactor volume and reaction pressure for crystal material synthesis [25]. Furthermore, several kinds of hierarchical self-sustaining macroscopic zeolite aggregates, such as hierarchical beta, ZSM-5, and EU-1 zeolite, had been fabricated currently by this dense gel steam conversion process [26–29]. In the present study, the predefined amorphous aluminum hydroxide (AAH) as precursor gels were transformed into self-sustaining Mg^{2+}, Al^{3+}-containing layered double hydroxide (MgAl–LDH) aggregates, forming a hierarchically meso/macroporous architecture via DGC without any surfactants and organic solvents. The formation process of LDH hierarchical pore structure, such as the evolution of phase composition, structure, and particle morphology during the whole process was investigated by using powder X-ray diffraction (XRD), scanning electron microscope (SEM), high-resolution transmission electron microscope (HRTEM), Fourier transform infrared (FT-IR), low-temperature N_2 adsorption–desorption, mercury intrusion, and inductively coupled plasma (ICP) emission spectrometry measurements. And, the formation mechanism was postulated based on the characterization results.

2 Experimental section

2.1 Preparation of AAH precursor

All the reagents were analytical grade and used without further purification. Ten grams of $Al(NO_3)_3 \cdot 9H_2O$ was first dissolved in 30 mL of deionized water under stirring at room temperature. Precipitation was performed by adjusting the pH of medium to 5.0 with 28 wt% ammonia aqueous solution. The gel solutions were poured into watch-glass and cured for 1 h and then dried at 20 Pa for 1 day by freeze drying. The white solid precipitates were collected and conserved in dryer.

2.2 Preparation of LDH hierarchical architecture by DGC method

In a typical DGC procedure, 0.10 g AAH precursor gel and 0.59 g anhydrous magnesium sulfate were ground into a well-distributed powder and transferred into a glass beaker in a Teflon vessel (200 mL), where 0.6 mL deionized water and 1.2 mL 28 wt% ammonia aqueous solution were poured at the bottom of the vessel and physically separated from the solid mixture. After the Teflon vessel was sealed and heated at 120 °C for different reaction time from 0.5 h

to 48 h, the obtained material was washed with deionized water and collected by centrifuging, then dried at 60 °C overnight.

Other experiment was undertaken in which Al $(NO_3)_3$•$9H_2O$ were used as Al precursor instead of AAH gel. Moreover, crystallization of AAH gel under the same conditions but in the absence of anhydrous magnesium sulfate were undertaken.

2.3 Preparation of LDH powder by coprecipitation method

For comparison, MgAl–LDH powder was synthesized by conventional coprecipitation method. A solution of 0.77 g $MgSO_4$ and 0.60 g $Al(NO_3)_3$•$9H_2O$ in 80 mL deionized water was poured into flask (250 mL), then added 15 mL 28 wt% ammonia aqueous solution, stirring quickly. The mixture was held at 70 °C for 24 h. The precipitate was separated by centrifugation, washed with water, and dried at 60 °C overnight.

2.4 Characterization of samples

The powder XRD measurements were performed on a Rigaku XRD-6000 diffractometer, using Cu Kα radiation ($\lambda = 0.15418$ nm) at 40 kV, 30 mA, with a scan step of 0.02° and a 2θ angle ranging from 3° to 70°. The morphology of the samples was investigated using a Hitachi S-3500N SEM with an accelerating voltage of 20 kV. HRTEM images were recorded with JEOL JEM-2010 transmission electron microscope. The accelerating voltage was 200 kV in each case. FT-IR spectrum was recorded in the region 4000–400 cm^{-1} on a Bruker Vector 22 spectrometer using KBr pellet technique. The N_2 sorption isotherms were measured using Micromeritics ASAP 2020 porosimeters at 77 K. The mesoporous specific surface area, pore-size distribution, and pore volume were calculated using the Brunauner–Emmett–Teller (BET) and Barrett–Joyner–Halenda (BJH) method, respectively. Hg-porosimetry analysis was performed on an Autopore IV 9510 porosimeter to measure macroporosity, with a maximum working pressure of up to 414 MPa, corresponding to pore diameters ranging from about 5 µm to 7 nm. Elemental analyzes were performed using a Shimadzu ICPs-7500 ICP emission spectrometer.

3 Results and discussion

MgAl–LDH architecture was fabricated by DGC method using home-made AAH gel and anhydrous magnesium sulfate as Al and Mg precursor materials, respectively. Aqueous ammonia was used as precipitating agent. Compared to XRD pattern of AAH precursor gel which shows an amorphous phase (Supporting Information Fig. S1a), the production sample prepared by DGC at 120 °C for 24 h presents a series of (00 *l*) diffraction lines at low 2θ values, characteristic of a layered structure (Fig. 1a). The (003) peak appears at 10.2° (the interlayer spacing $d_{003} =$ 0.86 nm), demonstrating the intercalation of sulfate anions into LDH gallery [30]. Besides, two broad asymmetric peaks around 35.6° and 61.4° corresponding to (012) and (110)/(113) reflection line were found in Fig. 1a, respectively, confirming a hexagonal lattice with a 3 R stacking of LDH layers [31]. The intercalation of sulfate anions into LDH interlayer can be further identified by FT-IR spectroscopy (Fig. 1b), showing the presence of a strong ν_3 mode of sulfate anions at 1118 cm^{-1} and a ν_4 mode at 614 cm^{-1} [30]. Besides, Fig. 1b shows that a strong absorption band centered around 3600 cm^{-1} can be identified as the hydroxyl stretching band $\nu(OH_{str})$, arising from metal hydroxyl groups and hydrogen-bonded interlayer water molecules. Another absorption band resulting from the hydroxyl deformation mode of water, $\delta(H_2O)$, is recorded at around 1645 cm^{-1}. Moreover, a small absorption band at ca. 1372 cm^{-1} and a should at ca. 837 cm^{-1} is attributed to the ν_3 and ν_4 mode of CO_3^{2-} ions, respectively, indicating the coexistence of a small amounts of CO_3^{2-} ions in the interlayer. The CO_3^{2-} ions maybe derived from the carbon dioxide gas in the reaction system. The effect of existence of carbonate on the formation mechanism of the hierarchically architecture of LDH is not clear at the present stage of study. In addition, the O–M–O bending mode of the hydroxide sheet is located at ca. 450 cm^{-1}. The Mg/Al molar ratio for the LDH product is about 3.1 identified by ICP.

Figure 1c shows a typical SEM image of an individual hierarchical LDH with irregular dimensions about of 11 × 8 µm. The self-sustaining LDH aggregates can be observed in the entire field of vision with the size in the range from a few to hundreds of microns. SEM image at a high-magnification (Fig. 1d) reveals the surface morphology of the particle which consists of a large number of nanoflakes intercrossed with each other. Meanwhile, SEM image of AAH precursor shows the agglomerates of amorphous gel particles with relatively smooth surface as well (Fig. S1c). The LDH crystallites present an orientation in which the *ab*-face of the platelets is normal to the surface of architecture. As revealed by the SEM image, LDH architecture exhibits a macroscopic pore network structure on the surface with relatively homogeneous macropore distribution about 100–200 nm in diameter. The interior feature of the hierarchical LDH material is demonstrated from a crushed particle sample (*inset* of Fig. 1c). LDH crystallites are aligned with a multilayer manner to form the network structure. The thickness of one LDH layer is about 1.2 µm.

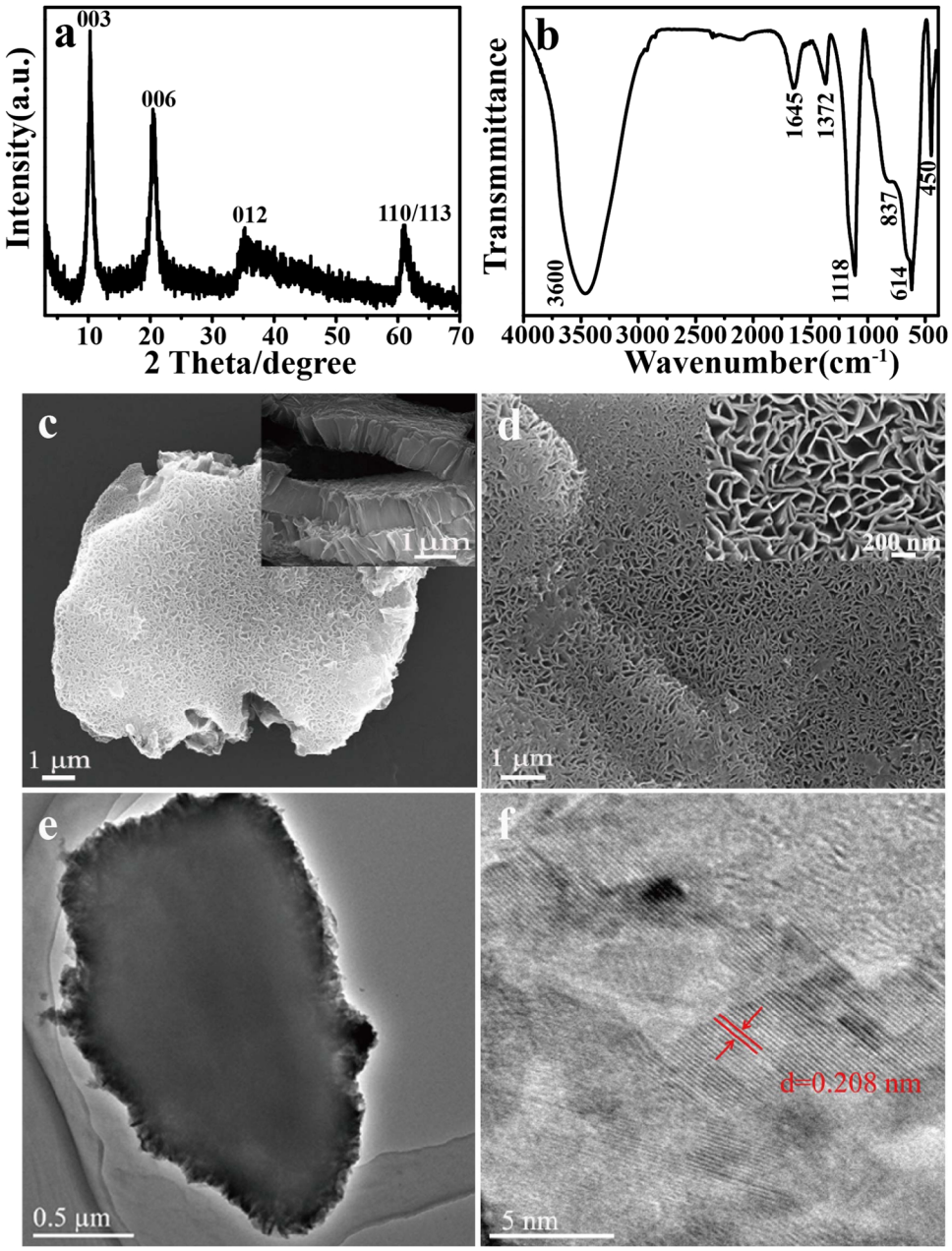

Fig. 1 XRD pattern (**a**), FT-IR spectrum (**b**), SEM images of low-magnification (**c**) and high-magnification (**d**), TEM (**e**), and HRTEM (**f**) images of hierarchical LDH obtained by DGC at 120 °C for 24 h. Inset of **c** shows the SEM image of a crushed particle indicating the interior feature

As a layered material, the sheet-like LDH crystallites are often observed to aggregate during crystallization, storage and application due to the high surface energy. A house-of-cards structure of LDH crystallites is commonly formed on a certain substrate by in situ growth in hydrothermal system [32], through hot water treatment of sol-gel-derived amorphous Al_2O_3–MgO film [33], or by electrodeposition [34]. The growth process and characteristics of the resulting film had been proved to be highly dependent on the nature and texture of the substrate material [35]. The LDH crystallites thus obtained in the LDH film were usually mono-layer arranged and well-oriented with their *ab*-faces perpendicular to the substrate. In our case, self-sustaining LDH architecture can be fabricated by DGC without the need of a substrate material, exhibiting a bi-modal porous structure having a macroporous network and a well defined mesoporous structure in the macroporous framework. In addition, LDH crystallites are arranged in a multilayer manner forming the architecture structure.

The morphology and structure features of LDH architecture were further confirmed by transmission elctron microscopy (TEM) observation (Fig. 1e). LDH sheets on the rim of architecture particle appear as needles, which may be due to the vertical orientation of the LDH primary

sheets to the Cu grid when stacking to form the architecture. Figure 1f of HRTEM image exhibits the lattice fringes of (211) plane with a lattice gap of 0.208 nm, providing further evidence of the appearance of LDH crystallite phase. On the contrary, Fig. S1d indicates the AAH precursor is amorphous. As demonstrated by lattice fringes all over the specimen in Fig. 1f, it is proposed that the LDH particles are completely crystallite throughout the sample.

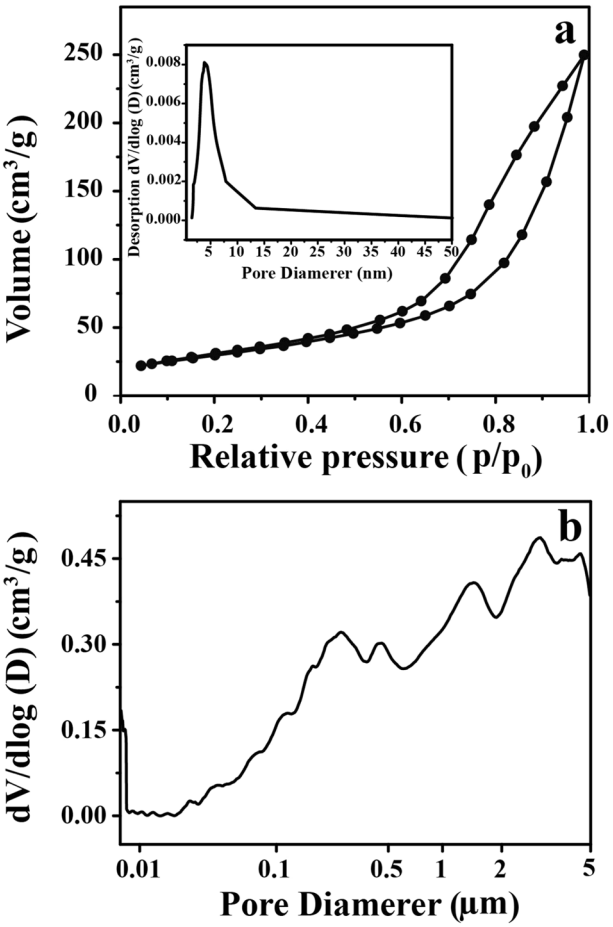

Fig. 2 Nitrogen sorption isotherm **a** and mercury intrusion porosimetry **b** of hierarchical LDH obtained by DGC at 120 °C for 24 h. Inset of **a** shows the corresponding pore size distribution of the hierarchical LDH sample

Figure 2a exhibits the N_2 adsorption isotherm of LDH architecture which displays a type-IV characteristic with a H_3-type hysteretic loop at the relative pressure ($p/p_0 > 0.4$), indicating the presence of a mesoporous structure. We can observe an inclination of the curve with the increase of pressure. According to the BJH calculation from desorption branch, the pore size distribution of LDH architecture shows a narrow size distribution in the mesopore range 3.2–4.8 nm with a sharp maximum at about 3.9 nm. However, we cannot clearly observe these mesopores from SEM and TEM images (Fig. 1). It is proposed that the mesopores maybe resulted from the platelet interstices of the LDH architecture structure. The BET specific surface area is calculated to be 107 m^2/g and a mesoporous volume of 0.403 cm^3/g (Table 1). Compared to AAH precursor sample (Fig. S2a), it is noticed a significant increase of specific surface area and mesoporous volume after DGC treatment. On the other hand, for the MgAl–LDH powder sample with Mg/Al molar ratio 3.0, which was synthesized by the conventional coprecipitation method using $MgSO_4$ and $Al(NO_3)_3 \cdot 9H_2O$ as raw materials (Fig. S3), the BET specific surface area is calculated to be 49 m^2/g and a mesoporous volume of 0.142 cm^3/g (Table 1). The relatively larger specific surface area for the self-sustaining LDH architectures may be attributed to the architecture structure with a large amount of hierarchical pores, which will give great contribution to the surface area when the amorphous particles are crystallized to LDH platelets.

In addition, we can see the continual increase in the adsorption volume of N_2 from relative pressures of 0.8 to 1.0 in Fig. 2a, suggesting that LDH architecture sample contains a large number of pores wider than ca. 50 nm.

Table 1 Evolution of textural properties characterized by nitrogen sorption and mercury porosimetry

sample	DGC time (h)	S_{BET}[a] (m^2/g)	V_{meso}[b] (cm^3/g)	V_{macro}[c] (cm^3/g)	pore diameter (N_2, BJH) (nm)	pore diameter (Hg-intrusion) (nm)
AAH gel	–	12	0.018	0.08	1.5	320
LDH architecture	4	36	0.188	0.5	1.8	220
LDH architecture	8	54	0.194	0.46	2.0 + 3.4	180
LDH architecture	24	107	0.403	0.62	3.9	150
LDH powder[d]	–	49	0.142	–	1.5	–

[a] The specific surface area is calculated according to the BET model from N_2 adsorption isotherms

[b] The mesoporous volume is calculated from N_2 adsorption isotherms at $P/P_0 = 0.989$

[c] The macroporous volume is taken from Hg porosimetry results in the range of porous diameters from 50 nm to 5 μm

[d] LDH powder sample prepared by coprecipitation method, using $MgSO_4$ and $Al(NO_3)_3 \cdot 9H_2O$ as raw materials and aqueous ammonia as precipitating agent (see Experimental section), is presented for comparison

Complementary mercury intrusion experiments enable the detection of macroscopic pores and the corresponding results of LDH architecture are displayed on Fig. 2b and Table 1. The macropore diameter was estimated over the whole mercury intrusion pressure range. The existence of main peak in the macropore range around 150 nm in diameter corresponds well to those revealed in the SEM image (Fig. 1c, d), from which we can clearly observe the pores of around diameter distribution of 100–200 nm on the surface. It is worthy noting that the main peak around 150 nm in diameter is absent for the AAH precursor sample (Fig. S2b). The high intrusion volume 0.62 cm^3/g indicates that these macropores are deeply penetrating three dimensionally in the LDH architectures. Meanwhile, the appearance of maropores larger than 1 μm in Fig. 2b may be attributed to the interparticle voids between LDH layers, which can be also seen in Fig. S2b, originating from spaces between the AAH aggregates.

To elucidate the evolution of the hierarchical LDH particles, we investigated the DGC procedure at 120 °C with different reaction time intervals. XRD patterns and SEM images of the specimens after synthesis treatment from 0.5 h to 48 h are shown in Fig. 3 and 4, respectively. Although XRD pattern of specimen synthesized with 0.5 h displays broad peaks characteristic of amorphous phase, SEM image shows the appearance of alveolate-like particles on the surface. We can see the weak (003) diffraction peaks of LDH material for specimen after 1 h. Concomitantly, SEM image shows that numerous nanoflakes curve from the particle surface. With the prolonging reaction time, the characteristic XRD diffraction peaks, such as (003), (012) and (110)/(113) peaks, gradually sharpen. Accordingly, a large number of plate-like LDH crystallites appear in the SEM images and the particle size increases gradually with the DGC treatment time.

The effects of reaction time on the evolution of textural properties of LDH architecture during DGC treatment were further investigated by N_2 sorption and mercury intrusion mercury intrusion experiments. N_2 physisorption measurement performed on AAH precursor gel results in a type I isotherm with a smaller porous volume of 0.018 cm^3/g (Fig. S2a and Table 1). After DGC treatment of AAH at 120 °C for 4 h, the type I isotherm is replaced by type IV isotherm characteristic of mesoporous solids (Fig. 5a). Accordingly, we can observe a significant increase of BET specific surface area and porous volume. The pore size distribution plot of the 4 h-specimen shows a pore peak at 1.8 nm. According to above observations on SEM images (Fig. 4), formation of a large number of plate-like LDH crystallites on the particle surface alter the initial porous structure of the AAH precursor gel. Further increase of crystallization time to 8 h leads to an enhanced specific surface area and porous volume. A bimodal pore size distribution centered at 2.0

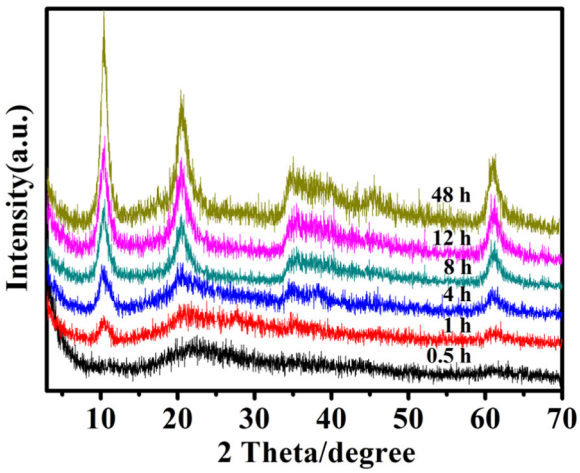

Fig. 3 XRD patterns of LDH hierarchical architectures obtained by DGC with different reaction times

and 3.4 nm for the 8 h-specimen has been noticed. It is worthy noting that the pore size distribution plot of the 24 h-specimen shows only one pore peak at 3.9 nm (Fig. 2), indicating the well crystallization and growth of LDH platelets under the employed reaction conditions. In addition, mercury porosimetry analyzes show the existence of main peak in the macropore range around 200 nm in diameter for the LDH architecture samples prepared with 4 and 8 h (Fig. 5b). Compared with that of the AAH gel, both LDH architectures exhibit a higher intrusion volume, resulting from the interparticle space between the aligned LDH crystallites.

To further identify the important role of the AAH precursor gel for the formation of LDH architecture, an additional experiment was carried out using $Al(NO_3)_3{\bullet}9H_2O$ and anhydrous magnesium sulfate as Al and Mg precursor material, respectively. A mixture of LDH and aluminum oxonium sulfate hydroxide ($(H_3O)Al_3(SO_4)_2(OH)_6$, JCPDS No. 16-0409) phase was obtained according to XRD of Fig. S4a. SEM of Fig. S4b further reveals the plate-like LDH crystallites with multifarious shapes are mixed with some aggregate particles of aluminum oxonium sulfate hydroxide. On the other hand, DGC procedure was conducted using only AAH gel and ammonia solution as raw materials, aluminum oxide hydroxide (AlOOH, JCPDS No. 49-0133) nanocrystals with rod-like morphology were formed (Fig. S5). In fact, when the obtaining AlOOH was used as raw material for DGC with anhydrous magnesium sulfate and ammonia solution in an additional experiment, no LDH crystals can be prepared under the identical reaction conditions for formation of LDH architecture. The above results suggest that the preformed AAH gel as raw material is necessary for induce the construction of LDH architecture with the employed synthesis conditions.

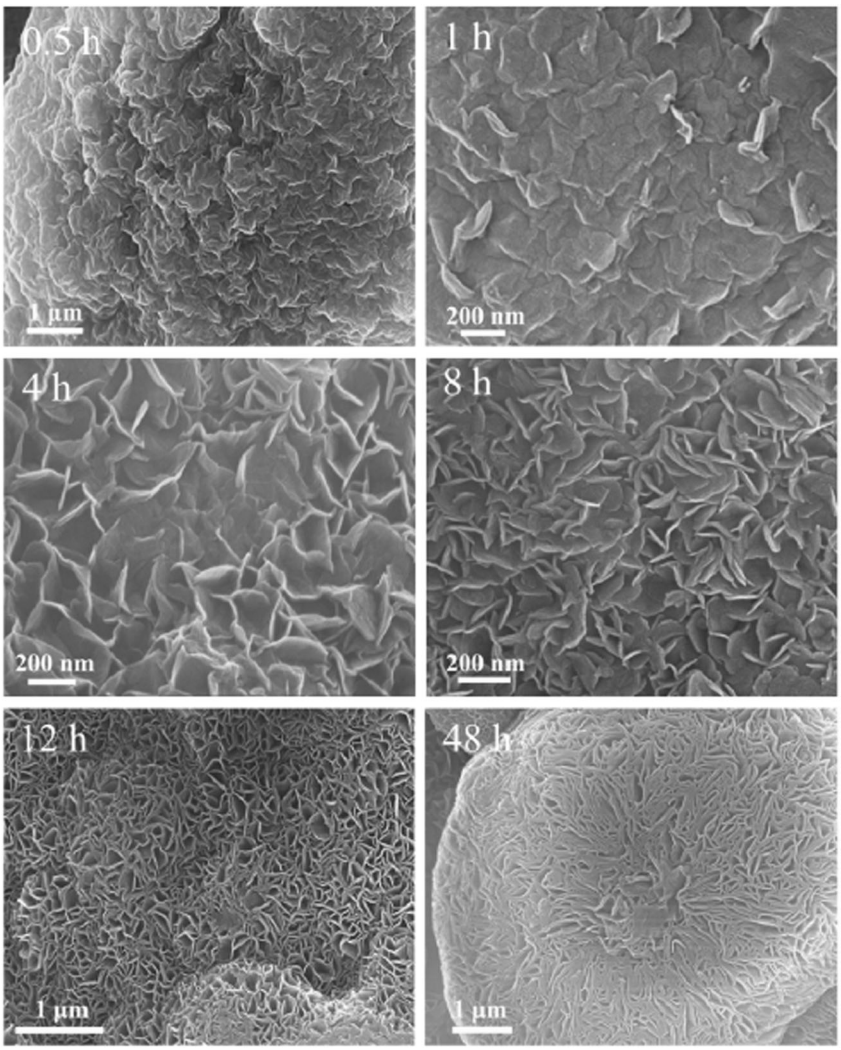

Fig. 4 SEM images of LDH hierarchical architectures obtained by DGC with different reaction times

According to the investigation on the formation procedure of MgAl–LDH crystal by precipitation method from magnesium and aluminum precursor salt solution using urea precipitating agent [36–38], amorphous colloidal hydroxide aluminum is observed to be formed initially from the aluminum precursor salt solution. Subsequently, the amorphous hydroxide is transformed into crystallites of oxide–hydroxide aluminum boehmite, accompanying the continuous incorporation of surrounding Mg^{2+} into the sheet for forming LDH crystallites. During the above solution-mediated LDH crystallization procedure, there is an equilibrium between the undissolved and dissolved Al species. The mobility of the dissolved species results in the nucleation and growth of LDH crystals at remote sites. Consequently, the resulting crystals have a different morphology from that of the initial AAH gel. In this case, during the initial steaming treatment, the dissociated Mg^{2+} from magnesium sulfate compound can incorporate with aluminum compound on the AAH surface or inside the interparticle voids where the mixed steam of volatile ammonia with water may permeate into because of the capillary effect. Then, positively charged brucite-like sheets forms using the distinctly MgO_6 and AlO_6 octahedral with plenty of surface-located OH^- groups, which should easily attract the negatively charged sulfate ions by electrostatic interaction. The nucleation of MgAl–LDH may be confined by suppressing the mobility of Al^{3+} species during crystallization. The continuously dissociation of the magnesium sulfate and the preorganized AAH material supply the necessary nutrients for the crystallization and growth of LDH nanoplatelets. Different from the growth of LDH crystal during the solution-mediate crystallization, LDH crystallization proceeds towards the AAH phase interior accompanying the continuous infiltration of the ammonia water steam, showing an inward growth of crystals during DGC process. Because the crystals with their fastest growth

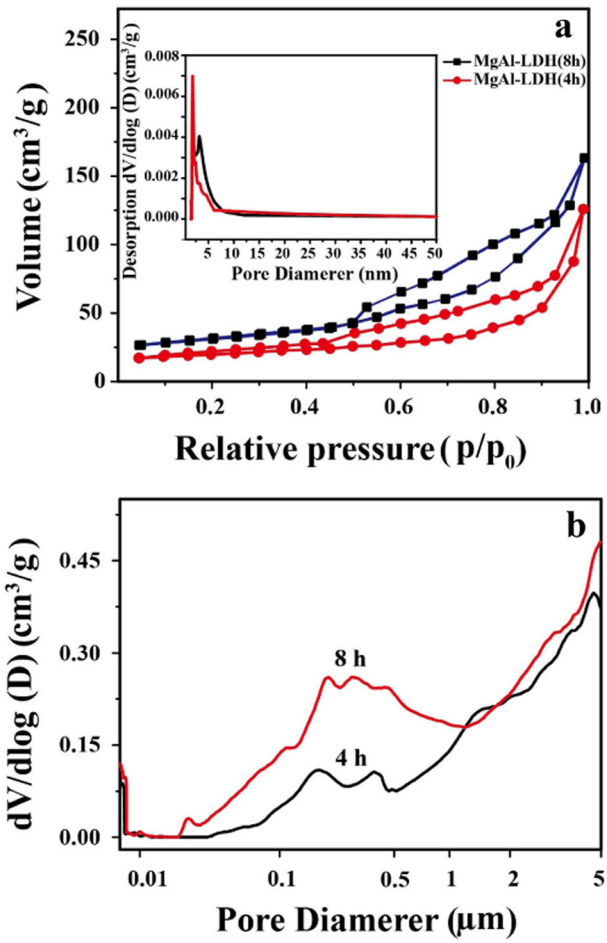

Fig. 5 N_2 sorption isotherms **a** and mercury intrusion porosimetry **b** of hierarchical LDH samples obtained by DGC with 4 and 8 h. *Inset* of **a** shows the corresponding pore size distribution of the two hierarchical LDH samples

direction (*ab*-direction) is normal to the AAH surface, the interlaced accumulation of LDH platelets restricts the growth by each other, exhibiting a final macroscopic pore network on the surface (Fig. 1c). The gradual increase in XRD reflection demonstrates that AAH phase is progressively transformed by a DGC treatment into a crystallite phase, resulting in a stable hierarchical bodies. Based on above experimental results, the formation mechanism of LDH architecture by DGC is proposed and represented schematically in Fig. 6.

4 Conclusions

In summary, a new type of hierarchical porous MgAl–LDH was fabricated by DGC method without the need of a surfactant and organic solvent. The resulting hierarchical LDH material exhibits a bi-modal porous structure having a macroporous network with macropore sizes of 100–200 nm and a well defined mesoporous structure of pore size around 3.9 nm in the macroporous framework. LDH crystallites are aligned with a multilayer manner to form the architecture structure. Compared to LDH powder sample, the self-sustaining LDH aggregates have a relatively larger specific surface area, which may be attributed to the architecture structure with a large amount of hierarchical pores. The DGC approach is facile and environmentally benign for fabrication of LDH hierarchical architectures, which are expected to be useful in many applications, such as catalysts, adsorbents, high-performance structural and functional devices, energy conversion, and bio-medical materials.

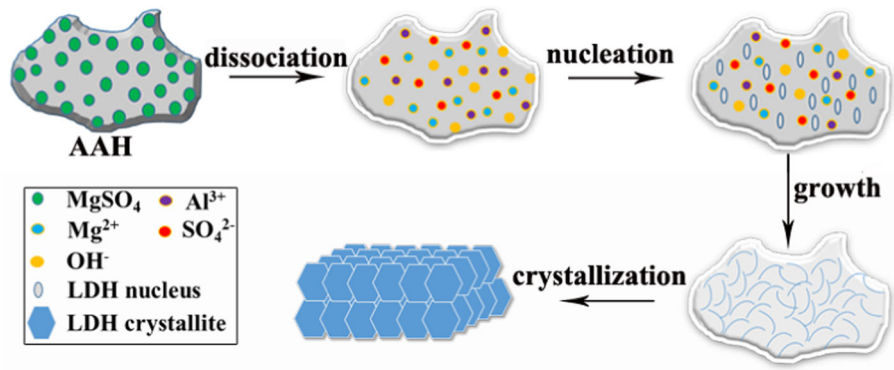

Fig. 6 Schematic illustration of a proposed evolution process of LDH hierarchical architecture by DGC. *Step 1*: dissociation of Mg^{2+} from magnesium sulfate compound aided by the ammonia solution steam atmosphere; *Step 2*: LDH nucleation occurring on the AAH surface or inside the interparticle voids where the ammonia solution steam could permeate into; *Step 3*: successive transformation of these LDH nuclei into nanocrystallites; at this stage, contraction and partial conversion of the AAH gel into nanocrystallites leading to an aggregated network with macrostructure from interparticle voids; and *Step 4*: transformation of numerous small crystallites into an final LDH hierarchically architecture with prolonged DGC treatment; the macropore size increases along with this particle growth

Acknowledgements This work was supported by the National Natural Science Foundation of China (No. 21376019, 21676013), the Fundamental Research Funds for the Central Universities (No. YS1406), and Beijing Engineering Center for Hierarchical Catalysts.

Compliance with ethical standards

Conflict of interest The authors declare that they have no competing interests.

References

1. Vaccari A (2001) Layered double hydroxides: present and future. Nova, Inc, New York, NY
2. Braterman PS, Xu ZP, Yarberry F (2004) Handbook of Layered Materials. Marcel Dekker, New York, NY
3. Williams GR, O'Hare D (2006) Towards understanding, control and application of layered double hydroxide chemistry. J Mater Chem 16:3065–3074
4. Evans DG, Slade RCT (2006) Structural aspects of layered double hydroxides. Springer Berlin Heidelberg. Struct Bond 119:1–87
5. Wang Q, O'Hare D (2012) Recent advances in the synthesis and application of layered double hydroxide (LDH) nanosheets. Chem Rev 112:4124–4155
6. Kuang Y, Zhao L, Zhang S et al. (2010) Morphologies, preparations and applications of layered double hydroxide micro-/nanostructures. Materials 3:5220–5235
7. Gunawan P, Xu R (2008) Synthesis of unusual coral-like layered double hydroxide microspheres in a nonaqueous polar solvent/surfactant system. J Mater Chem 18:2112–2120
8. Prevot V, Caperaa N, Taviot-Gueho C et al. (2009) Glycine-assisted hydrothermal synthesis of NiAl-layered double hydroxide nanostructures. Cryst Growth Des 9:3646–3654
9. Shao M, Ning F, Zhao J et al. (2013) Hierarchical layered double hydroxide microspheres with largely enhanced performance for ethanol electrooxidation. Adv Funct Mater 23:3513–3518
10. Li L, Ma R, Iyi N et al. (2006) Hollow nanoshell of layered double hydroxide. Chem commun 42:3125–3127
11. Gunawan P, Xu R (2009) Direct assembly of anisotropic layered double hydroxide (LDH) nanocrystals on spherical template for fabrication of drug-LDH hollow nanospheres. Chem Mater 21:781–783
12. Li L, Feng Y, Li Y et al. (2009) Fe_3O_4 core/layered double hydroxide shell nanocomposite: versatile magnetic matrix for anionic functional materials. Angew Chem 121:6002–6006
13. Géraud E, Prévot V, Ghanbaja J et al. (2006) Macroscopically ordered hydrotalcite-type materials using self-assembled colloidal crystal template. Chem mater 18:238–240
14. Géraud E, Rafqah S, Sarakha M et al. (2008) Three dimensionally ordered macroporous layered double hydroxides: preparation by templated impregnation/coprecipitation and pattern stability upon calcination. Chem Mater 20:1116–1125
15. Whitesides GM, Grzybowski B (2002) Self-assembly at all scales. Science 295:2418–2421
16. Xu L, Ma W, Wang L et al. (2013) Nanoparticle assemblies: dimensional transformation of nanomaterials and scalability. Chem Soc Rev 42:3114–3126
17. Chang CC, Cho HJ, Wang Z et al. (2015) Fluoride-free synthesis of a Sn-BEA catalyst by dry gel conversion. Green Chem 17:2943–2951
18. Chen B, Huang Y (2011) Formation of microporous material $AlPO_4$-18 under dry-gel conversion conditions. Microporous Mesoporous Mater 143:14–21
19. Naik SP, Chiang AST, Thompson RW (2003) Synthesis of zeolitic mesoporous materials by dry gel conversion under controlled humidity. J Phys Chem B 107:7006–7014
20. Matsukata M, Ogura M, Osaki T et al. (1999) Conversion of dry gel to microporous crystals in gas phase. Top Catal 9:77–92
21. Xu W, Dong J, Li J et al. (1990) A novel method for the preparation of zeolite ZSM-5. J Chem Soc Chem Commun 10:755–756
22. Matsufuji T, Nishiyama N, Ueyama K et al. (2000) Permeation characteristics of butaneisomers through MFI-type zeolitic membranes. Catal Today 56:265–273
23. Alfaro S, Arruebo M, Coronas J et al. (2001) Preparation of MFI type tubular membranes by steam-assisted crystallization. Microporous Mesoporous Mater 50:195–200
24. Shi Q, Chen Z, Song Z et al. (2011) Synthesis of ZIF-8 and ZIF-67 by steam-assisted conversion and an investigation of their tribological behaviors. Angew Chem Int Ed 50:672–675
25. Meng X, Xiao FS (2014) Green routes for synthesis of zeolites. Chem Rev 114:1521–1543
26. Möller K, Yilmaz B, Jacubinas RM et al. (2011) One-step synthesis of hierarchical zeolite beta via network formation of uniform nanocrystals. J Am Chem Soc 133:5284–5295
27. Han SW, Kim J, Ryoo R (2017) Dry-gel synthesis of mesoporous MFI zeolite nanosponges using a structure-directing surfactant. Microporous Mesoporous Mater 240:123–129
28. Li H, Jin J, Wu W et al. (2011) Synthesis of a hierarchically macro-/mesoporous zeolite based on a micro-emulsion mechanism. J Mater Chem 21:19395–19401
29. Goergen S, Guillon E, Patarin J, Rouleau L (2009) Shape controlled zeolite EU-1 (EUO) catalysts: dry gel conversion type synthesis, characterization and formation mechanisms. Microporous Mesoporous Mater 126:283–290
30. Kloprogge JT, Wharton D, Hickey L, Frost RL (2002) Infrared and Raman study of interlayer anions CO_3^{2-}, NO_3^-, SO_4^{2-} and ClO_4^- in Mg/Al-hydrotalcite. Am Mineral 87:623–629
31. Faour A, Mousty C, Prevot V et al. (2012) Correlation among structure, microstructure, and electrochemical properties of NiAl-CO_3 layered double hydroxide thin films. J Phys Chem C 116:15646–15659
32. Chen HY, Zhang FZ, Chen T, Xu SL, Evans DG, Duan X (2009) Comparison of the evolution and growth processes of films of M/Al-layered double hydroxides with M=Ni or Zn. Chem Eng Sci 64:2617–2622
33. Yamaguchi N, Ando D, Tadanaga K, Tatsumisago M (2007) Direct formation of Mg-Al-layered double hydroxide films on glass substrate by the sol-gel method with hot water treatment. J Am Ceram Soc 90:1940–1942
34. Nguyen T, Boudard M, Carmezim MJ, Montemor MF (2017) $Ni_xCo_{1-x}(OH)_2$ nanosheets on carbon nanofoam paper as high areal capacity electrodes for hybrid supercapacitors. Energy 126:208–216
35. Guo XX, Zhang FZ, Evans DG, Duan X (2010) Layered double hydroxide films: synthesis, properties and applications. Chem Commun 46:5197–5210
36. Fogg AM, Williams GR, Chester R, O'Hare D (2004) A novel family of layered double hydroxides-$[MAl_4(OH)_{12}](NO_3)_2{\cdot}xH_2O$ (M=Co, Ni, Cu, Zn). J Mater Chem 14:2369–2371
37. Seron A, Delorme F (2008) Synthesis of layered double hydroxides (LDHs) with varying pH: a valuable contribution to the study of Mg/Al LDH formation mechanism. J Phys Chem Solids 69:1088–1090
38. Yang YM, Zhao XF, Zhu Y, Zhang FZ (2012) Transformation mechanism of magnesium and aluminum precursor solution into crystallites of layered double hydroxide. Chem Mater 24:81–87